Chemical Engineering Journal 108 (2005) 81–90

Chemical Engineering Journal

www.elsevier.com/locate/cej

Scale up study of retreat curve impeller stirred tanks using LDA measurements and CFD simulation

Mingzhong Li[a,*], Graeme White[a], Derek Wilkinson[a], Kevin J. Roberts[b]

[a] *Department of Chemical Engineering, School of Engineering and Physical Sciences, Heriot-Watt University, Edinburgh EH14 4AS, UK*
[b] *Institute for Particle Science and Engineering, Department of Chemical Engineering, University of Leeds, Leeds LS2 9JT, UK*

Received 22 June 2004; received in revised form 5 January 2005; accepted 12 January 2005

Abstract

In this paper, scale up effects have been investigated for three geometrically similar laboratory scale vessels of 0.5, 2 and 20 l with retreat curve impellers and cylindrical baffles, which mimic reactors widely used in the pharmaceutical and fine chemical industries, using CFD simulations. The convergence of fully three-dimensional, time-dependent numerical computations has been monitored to ensure the simulations reached quasi-steady state. CFD results have then been validated using LDA measurements and empirical power consumption literature data. The comparisons of power number, discharge flow number, secondary circulation flow number and pumping efficiency at three different scales suggest that the selection of scale of a laboratory vessel has little effect on the macro mixing performance for optimisation of the configuration and operating conditions of an industrial scale reactor.

Keywords: CFD simulations; LDA measurements; Scale up; Retreat curve impeller

1. Introduction

Stirred tanks are widely used in industrial mixing processes, especially in the fine chemicals and pharmaceuticals industries. The scale up of mixing tanks from laboratory to plant size is a crucial issue in the design of industrial processes to find optimal configurations and operating conditions. Normally, laboratory scale experiments can be carried out easily and the effects of tank geometry and process parameters can be studied at low cost. These results are then used to scale laboratory size up to industrial size, reducing or eliminating the high costs and difficulties of performing research on full-scale plants. However, scale up of stirred tanks from laboratory scale to pilot and full-scale plant is not straightforward. Depending on the physical process limiting the performance of the mixing vessel, it is commonly suggested that at least one of the mixing characteristics such as power input per unit volume, impeller discharge flow, impeller tip speed, Weber number, and Reynolds number, should be maintained constant [1]. The most significant problem in scale up occurs when different physical processes become limiting at different scales. Industrial scale reactors must perform several functions simultaneously (dispersion, reaction, and heat transfer) which do not scale up in the same manner. Thus the scale up of mixing tanks directly from laboratory to industrial scale is not always successful. On the other hand, the choice of a laboratory scale reactor for experiments is another aspect which should be investigated because the results from different laboratory scale vessels may directly affect the optimisation of the industrial scale reactor's operating parameters. The object of this paper is to investigate the macro mixing performance of different laboratory scale vessels.

In this work, three different laboratory scale vessels, each of them equipped with a retreat curve impeller and a cylindrical baffle, have been used for scale up study. These are all scaled down from a 63 l industrial pilot reactor with the same system configuration (DIN 28146). The retreat curve impeller is widely used in fine chemical and pharmaceutical production. However, unlike Rushton turbine and pitched blade impellers [2–11], it has not been given much atten-

* Corresponding author. Tel.: +44 131 451 3778; fax: +44 131 451 3129.
E-mail address: mingzhong.li@hw.ac.uk (M. Li).

1385-8947/$ – see front matter © 2005 Elsevier B.V. All rights reserved.
doi:10.1016/j.cej.2005.01.005

tion. An exception is the work by Campolo et al. [12,13], in which numerical simulations were used to characterise the fluid dynamic behaviour of two different industrial size reactors (12,500 l) and a laboratory scale reactor (30 l) with a retreat curve impeller or turbofoil turbine, predicting the macro mixing performances of power consumption and pumping efficiency. However, a rigorous experimental validation has not yet been made except that the power consumption in the reactor simulation was compared with the experiments.

The three scale vessels in this study are 0.5, 2 and 20 l which are geometrically similar, thus the effect of different scale up criteria can be investigated and evaluated. The macro mixing characteristic is one of the most interesting aspects for the scale up of a reactor because it affects general mixing performance as well as mass transfer properties in the reactor. Power number, pumping capacity, pumping efficiency and secondary circulation flow number were evaluated as functions of the Reynolds number. The data for the comparisons were generated from fully three-dimensional, time-dependent numerical computations of the flow field since computational fluid dynamics (CFD) is now a practical way to analyse the flow in stirred vessels, providing a rich and detailed level of information throughout the whole vessel. The simulations were carried out by a commercial CFD package (CFX5.5.1) using unstructured meshes with a 'sliding-mesh' technique to predict flow characteristics for different scale vessels [14]. In view of the lack of experimental data for a stirred vessel with a retreat curve impeller, Laser Doppler Anemometer (LDA) measurements for the velocities in the 20 l vessel and a comparison of power consumption in different scale vessels with literature data by Nagata [15] have been done to validate the CFD results, proving that the scale up study using CFD simulation is legitimate.

2. Methodologies

2.1. CFD simulations

Full three-dimensional, time-dependent simulations were performed for the different scale vessels at 0.5, 2 and 20 l, each of them equipped with a retreat curve impeller and a cylindrical baffle, using the computational fluid dynamics code CFX version 5.5.1. This is a finite volume based computational fluid dynamics analysis program which solves the non-linear set of equations formed by the discretisation of the Navier–Stokes conservation equations. The three scale vessels are geometrically similar. The system configuration is shown in Fig. 1 and the dimensional data are listed in Table 1. The dimensions of the system are scaled down from a standard 63 l reactor (DIN 28146). The curved shape of the vessel bottom allows the impeller to be placed very close to the bottom making the reactor suitable for suspending heavy dispersions effectively. The single cylindrical baffle was used to mimic the finger baffles found in conventional glass lined stirred reactors to improve the top–bottom turnover. The retreat angle formed by retreat curve impeller blades is 15°, the same for all scale vessels. As all simulations were run in the turbulent regime, turbulence was modelled using the SST (Shear-Stress-Transport) model [16], which is a combination of the k–ω model near the wall and the k–ε model away from the wall. In this way, both models are used in areas where they perform best. The CFX code allows the use of unstructured meshes for modelling complex geometries with local mesh refinement. In each simulation, the computational mesh was made up of two parts: an inner rotating cylindrical volume enclosing the retreat curve impeller and an outer stationary volume containing the rest of the vessel. The sliding mesh procedure was applied, in which the rotating mesh slid relative to the stationary mesh. The location of the interface between the volumes was selected at the middle of the gap between the impeller tip and the inside edge of the baffle so that the region of flow periodicity was contained within the sliding mesh. An illustration of the inner and outer meshes is given in Fig. 2, which clearly shows that finer meshes have been formed around the impeller and baffle regions, where the velocity spatial gradients are expected to be large. The boundary condition of no-slip velocity was applied to all liquid–solid boundaries. The free surface was

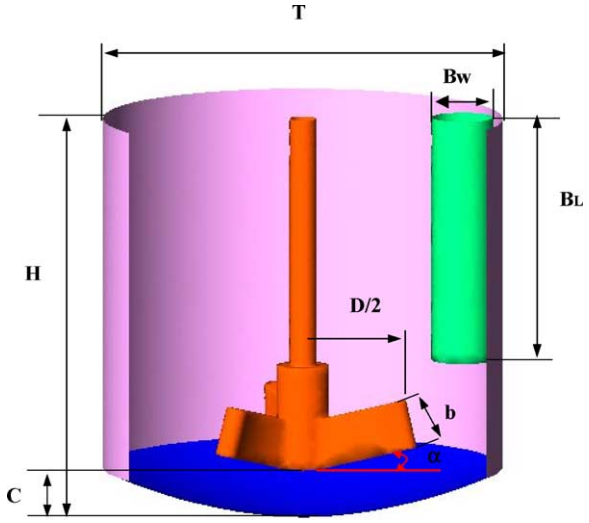

Fig. 1. Stirred reactor configuration.

Table 1
Dimensions of vessel and impeller used for scale up study

	20 l vessel	2 l vessel	0.5 l vessel
Tank diameter, T (mm)	294	148	90
Liquid height, H (mm)	294	148	90
Liquid volume, V (l)	18.31	2.31	0.52
Baffle width, BW (mm)	48	24	14
Baffle length, BL (mm)	183	92	55
Number of baffles, n_B	1	1	1
Impeller diameter, D (mm)	174	87	52
Impeller clearance, C (mm)	33	17	11
Blade width, B (mm)	34	17	11
Number of blades, n_b	3	3	3
Blade angle, α (°)	15	15	15

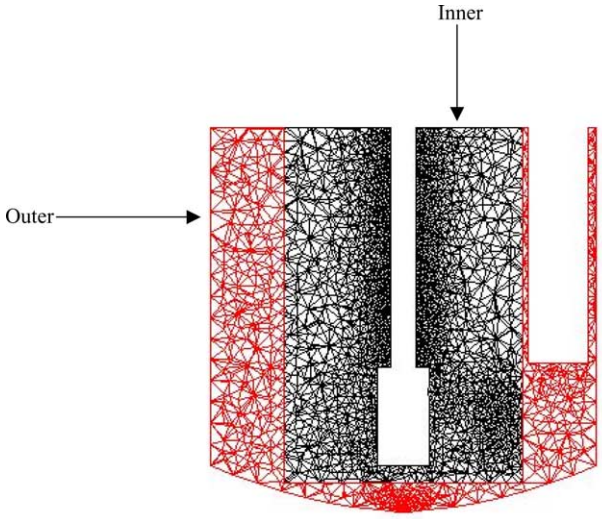

Fig. 2. Illustration of computational mesh.

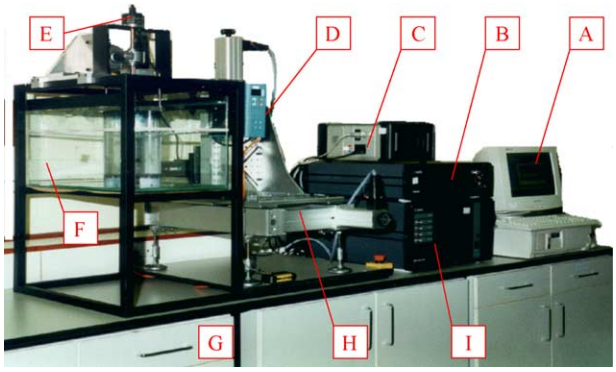

Fig. 3. Configuration of LDA experimental system: (A) computer; (B) laser generator; (C) traverse system controller; (D) stirrer motor controller; (E) stirrer encoder; (F) glass tank; (G) reactor; (H) 3D traverse system; (I) flow velocity analyser.

set on the top of the liquid in the vessel as a zero shear flat wall interface. The CFD model for the mixing vessel does not require any input of velocity field or other empirical parameters within the impeller sweep volume therefore reducing error associated with uncertainty of measured initial values.

Firstly, grid independence analyses [17] have been done to achieve unique results for each scale vessel. The number of nodes and cells used in each simulation to get grid independent results is shown in Table 2.

In order to give good initial values for a transient simulation, a steady state simulation was first run using the frozen rotor frame change model, producing a steady state solution to the multiple frame of reference problem and ignoring the transient effects at the frame change interface, to deal with the interaction of the flow between inner and outer portions of the computational grid. This technique is useful for obtaining results quickly in situations with a significant degree of symmetry. The subsequent transient simulation was carried out with a small time step corresponding to 1/120 of the impeller revolution period, which was the optimal time step [5,12–14,17]. In the sliding mesh procedure, the transient rotor–stator frame change model, accounting for transient interaction effects at a sliding (frame change) interface to obtain all interaction effects between components that are in relative motion to each other, was used, which predicts the true transient interaction of the flow between a stator and rotor passage. Total simulation running time corresponding to 10 impeller revolutions was set for each simulation, which is shown in the next section to be enough to allow the solution to reach quasi-steady state. The simulation was run on a Pentium IV processor with 1.0 Gb memory, 2.8 GHz clock frequency under the Windows 2000 operating system.

2.2. LDA experiments

Experiments have been done to measure the velocity distribution in a 20 l vessel using LDA to validate the CFD results. The stirred vessel used in the experiment was made from glass with a curved bottom equipped with a cylindrical baffle and a retreat curve impeller. The system configuration is the same as that of the 20 l vessel simulation shown in Fig. 1. The experimental system is shown in Fig. 3. The detailed experimental procedure can be found in the paper [17]. The LDA measurements were carried out on a plane which is 60° downstream of the cylindrical baffle shown in Fig. 4(a). On this plane, a total of 66 points, shown in Fig. 4(b), were selected around the impeller. Measurements were conducted at 100 rpm impeller rotation speed.

3. Results

In this section, the convergence of the simulations is first monitored to ensure the CFD results reach quasi-steady state. Then the CFD simulation results are validated using the LDA measurements and a power characteristic curve by Nagata [15]. Finally the scale up study is carried out using the CFD simulations for different scale vessels at 0.5, 2 and 20 l.

Table 2
Node and cell numbers in each simulation

	0.5 l vessel		2 l vessel		20 l vessel	
	Inner	Outer	Inner	Outer	Inner	Outer
Number of nodes	29877	13126	44055	13085	63232	12685
Number of tetrahedrons	163266	65849	241808	65439	344403	62554

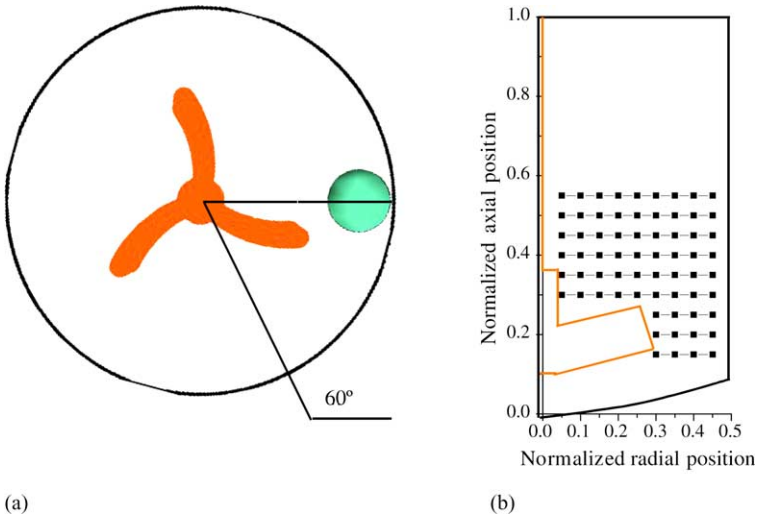

Fig. 4. Measurement plane and points: (a) measurement plane; (b) measurement points.

3.1. Convergence to quasi-steady state

All the simulations in this study are assumed to reach quasi-steady state. Once an impeller is set at a constant rotation speed in a still fluid, after a few impeller revolutions, the flow field becomes quasi-steady state in which the flow field averaged over one cycle is time independent. The quasi-steady state is easy to achieve under the experimental conditions after several impeller revolutions. However, the computing effort to achieve the quasi-steady state is variable for different CFD simulations, depending on the grid density and initial values of a transient simulation. In our study, the initial values of a transient simulation come from a corresponding steady state simulation. Thus, the running time of the simulation to reach the quasi-steady state is greatly reduced, compared with the normal order of 30–40 impeller revolutions required to reach the quasi-steady state [12,13]. In the simulations, two different flow variables, the upward flow rate and power consumption in the vessel, were monitored to ensure each of them reached the quasi-steady state.

The upward mass flow rate (upflow) w_{up} is defined as the integral across a section normal to the rotation axis of upward directed fluxes,

$$w_{up} = \int_{A^+} \rho V \, dA_z = \int_{A^+} \rho v_z \, dA_z \quad (1)$$

where V is the velocity, ρ the density, A_z the section normal to the rotation axis, and A^+ the portion of the section normal to the rotation axis where the axial component of velocity, v_z, is directed upward. This variable can also be used to measure the stirring capability of the reactor in the vertical direction called secondary circulation flow. Fig. 5 shows the upward flow rate distribution with vertical position and evolution of the upward flow rate with impeller revolutions for 20, 2 and 0.5 l vessels at 100 rpm impeller rotation speed. The upward flow rate in each vessel is unsteady at the initial values. As the flow develops, the upward flow profile progressively reaches a steady state, which means that the solution has reached a quasi-steady state. As good initial values were provided for each transient simulation, it took around 10 revolutions to reach the quasi-steady state. From Fig. 5, it can also be seen that the upward flow profiles are quite similar for different scale vessels, which means that the upward flow rate distribution is the same for geometrically similar stirred vessels. The upward flow rate gradually increases with vertical position and reaches a peak around 0.38 T, and then it gradually decreases.

Power consumption is another crucial characteristic of stirred-tank reactors, which is calculated from the total dissipation of power in the entire fluid volume. The power consumption P is calculated as the product of torque on the impeller blades and shaft with the angular velocity [10],

$$P = \omega \int_A r \times (\tau \, dA) \quad (2)$$

where A is the overall impeller and shaft surface area, ω the angular velocity vector, r the position vector, and τ the stress tensor.

The evolution of the power consumption in each simulation is shown in Fig. 6. From these curves, it can be seen that the power reaches a peak and then quickly decreases toward a constant value, which is different from the findings by Campolo et al. [12] in which a slow decay was found towards the final steady state. The main reason for the difference may come from the different initial values used in simulations. It took 10 iterations for the power to achieve steady state, which is the same as the evolution of the upflow profile.

Eight different simulations for each scale vessel at the same Reynolds numbers have been run for the scale up study.

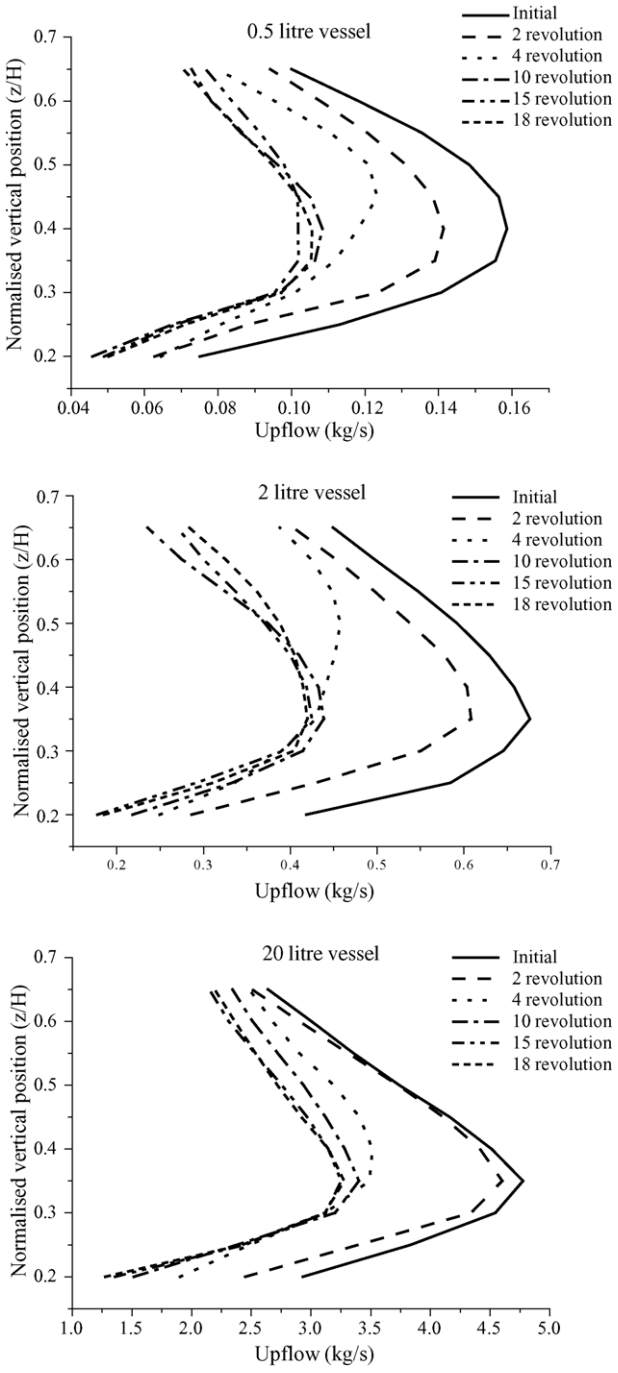

Fig. 5. Evolution of upflow profile.

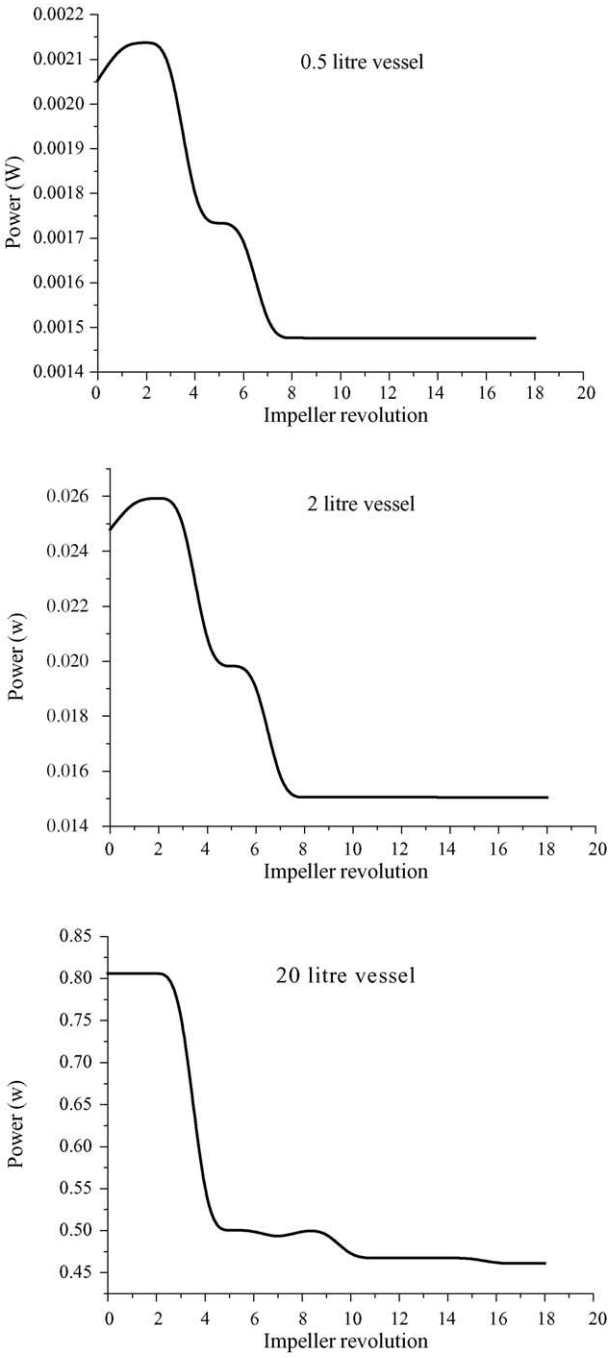

Fig. 6. Evolution of power input.

The Reynolds number in a stirred tank is defined as

$$Re = \frac{\rho N D^2}{\mu} \quad (3)$$

where N is the angular velocity, D the impeller diameter and μ the fluid viscosity.

For each simulation, a steady state simulation was first run with the target residual 10^{-4}, whose results were used as the initial values for the transient simulation with running time corresponding to 10 impeller revolutions which have been proven to be enough for the simulation to reach the quasi-steady state.

3.2. CFD validation

3.2.1. Power number validation

To validate the CFD results, the power numbers calculated by CFD simulations are compared with correlations by Na-

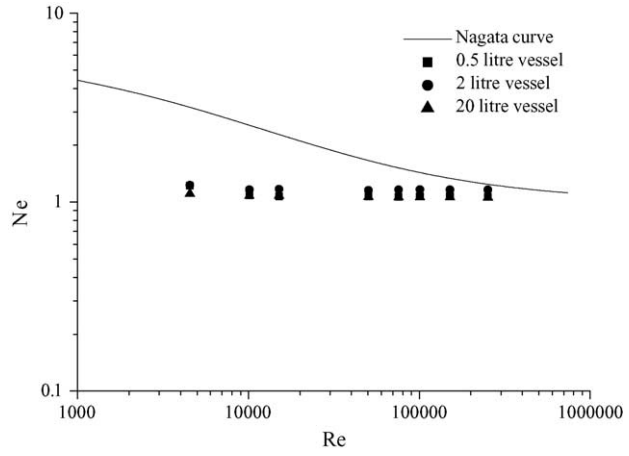

Fig. 7. Power number comparison.

gata [15]. The dimensionless power number can be calculated using the power consumption into the vessel, P, by

$$N_{\mathrm{p}} = \frac{P}{\rho N^3 D^5} \tag{4}$$

The semiempirical power characteristic curve by Nagata is widely used to calculate the stirred tank power number [10,12,13], showing very good agreement between the predictions and experiments. Detailed calculation of the power number curve is given by Nagata [15] and Campolo et al. [12,13]. As the geometries are similar for the three different scale vessels, the power characteristic curves are the same as shown in Fig. 7. Nagata's power curve shows that the power number becomes independent of the Reynolds number in the region of $Re > 10^5$, but this is not appropriate for the geometry used here because the power number should become independent of Re in the turbulent region, $Re > 10^4$, as shown in previous works [12,13]. The failure of the power number prediction by Nagata is due to the larger baffle diameter to tank diameter ratio in this work. However, the empirical expression can still be used to predict the power number in the region of $Re > 10^5$.

The power numbers calculated from the simulation results at different Reynolds numbers are also shown in Fig. 7. Overall, a good agreement between simulation and prediction results is found when the Reynolds number is beyond 10^5. The empirical prediction of power number is 1.02 and calculations of power number are 1.07, 1.16 and 1.06 for the 0.5, 2 and 20 l vessels respectively. The calculation of the power number for the 2 l vessel simulation has the biggest error about 12% in contrast to 5% for the 0.5 l vessel simulation and 4% for the 20 l vessel simulation. In previous works [12,13], the empirical prediction of the power number by Nagata is 0.866 for the retreat curve impeller agitated reactor with two baffles and accuracy of ±8% was found for the power number comparison given by the experimental data and CFD simulations. Furthermore, the CFD

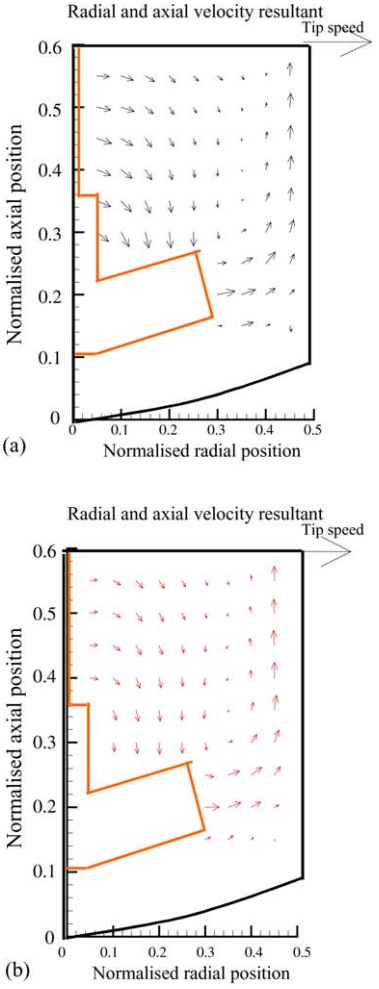

Fig. 8. Flow pattern comparison for 20 l vessel. (a) LDA measurements; (b) CFD prediction.

simulation predicts power number in the turbulent region, $Re > 10^4$, to be independent of Reynolds number, which is as expected.

3.2.2. Flow pattern validation using LDA measurements

The CFD simulation results were further validated by LDA measurements in this study. The LDA measurements were conducted in a 20 l vessel at 100 rpm impeller rotation speed. LDA measured velocities presented in the comparison are phase-averaged measurements. The mean velocities from the CFD simulation were averaged over one revolution of simulated rotation angle of the impeller and measurement points were the same locations as those in the LDA measurements. The flow field predicted by the CFD simulation is compared with experimental LDA results in Fig. 8 presented in the form of vectors which represent the resultant axial and radial velocities normalised by the impeller tip speed. Overall features of the flow field on the plane plotted by the LDA data are correctly reproduced by the CFD simulation. A radial flow prevails in the region be-

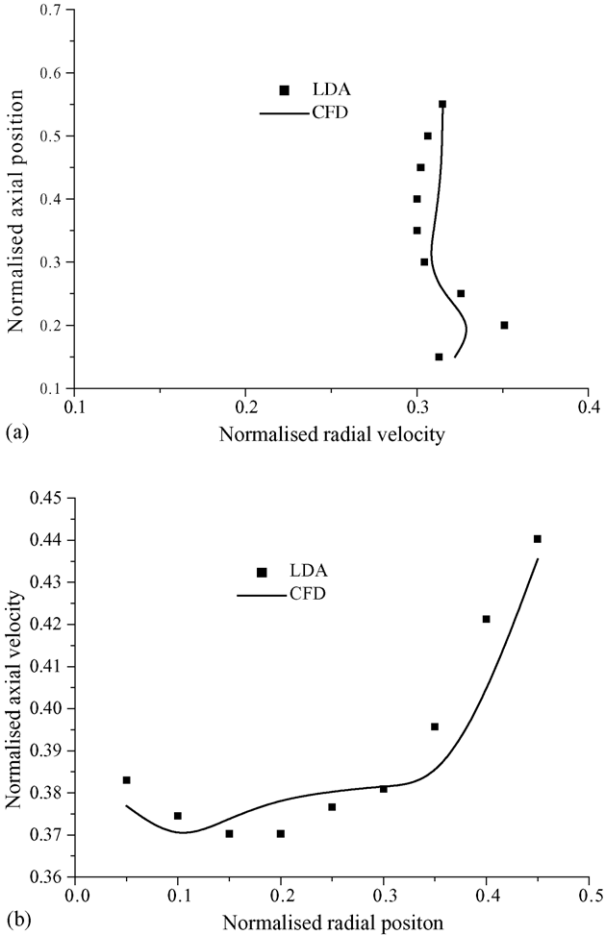

Fig. 9. Radial and axial velocity comparison. (a) Radial velocity comparison at $r/T = 0.3$. (b) Axial velocity comparison at $z/H = 0.4$.

tween the impeller blade tip and the vessel wall and there is an upward flow near the vessel wall. A vortex is created above the tip of the impeller and a strong downward axial flow is induced towards the impeller region between the impeller shaft and blade tip. The shape and magnitude of the flow and vortex centre are satisfactorily predicted. Quantitative comparisons of axial and radial velocities are given in Fig. 9. Fig. 9(a) shows the radial velocity comparison at $r/T = 0.3$ and Fig. 9(b) shows the axial velocity comparison at $z/T = 0.4$. The maximum prediction error between the LDA measurements and CFD predictions is about 8% within the experimental error (±10% of the tip speed), proving that CFD simulation is suitable for stirred tank scale up study.

3.3. Scale up study

Macro mixing performance comparisons including power number, flow number, secondary flow number and pumping efficiency are given at the three scales.

3.3.1. Power number comparison

Power number N_p is defined by Eq. (4). A comparison is given in Table 3 for each vessel scale at eight Reynolds numbers. The results show that power number is constant when Reynolds number is larger than 10^4 for all vessel scales. The power numbers of 1.07 for the 0.5 l and 1.06 for the 20 l vessels are in close agreement in contrast to the power number of 1.16 for the 2 l vessel. In previous works [12,18], it was found that power number slightly increases with tank scale. In this work, a dependence of power number on vessel size was found, but not the same tendency. As yet, this is unexplained but it may be due to different system configurations or CFD simulations.

3.3.2. Pumping capacity comparison

Pumping capacity is the flow rate that crosses the impeller plane and is the crucial variable in evaluating circulation in the reactor, which depends on the geometrical configuration of the vessel. Because the retreat curve impeller acts mainly as a radial impeller, the impeller flow can be calculated by integrating the radial component of the velocity, v_r, on the minimal cylindrical surface coaxial with the impeller enclosing the blades as follows,

$$w_d = \int_{A_r} \rho V \, dA_r = \int_{z_b}^{z_t} 2\pi\rho R_b v_r \, dz \tag{5}$$

where A_r is the cylindrical surface of radius R_b, z_b the impeller bottom height and z_t the impeller top height. The cylindrical surface for the calculation of impeller flow at each scale is shown in Fig. 10, in which the normalised diameter $R_b/T = 0.32$ and the normalised vertical distances $z_b/H = 0.1$ and $z_t/H = 0.3$ were selected. The discharge flow can be represented by the dimensionless impeller flow number by

$$N_d = \frac{w_d}{\rho N D^3} \tag{6}$$

A comparison of flow number at different scales is given in Table 3. Flow number slightly decreases with Reynolds number and tends to be constant at $Re > 5.0 \times 10^4$ for each scale vessel. The flow number significantly depends on vessel scale, which decreases with increasing vessel size.

3.3.3. Pumping efficiency comparison

Pumping efficiency is the pumping capability per unit of power consumed, defined as

$$\eta = \frac{N_d}{N_p} \tag{7}$$

A comparison of pumping efficiency at different scales is given in Table 3. The pumping efficiency is nearly independent of Reynolds number according to the simulations for each scale vessel. The pumping efficiency is a function of vessel size and tends to be smaller for a large vessel.

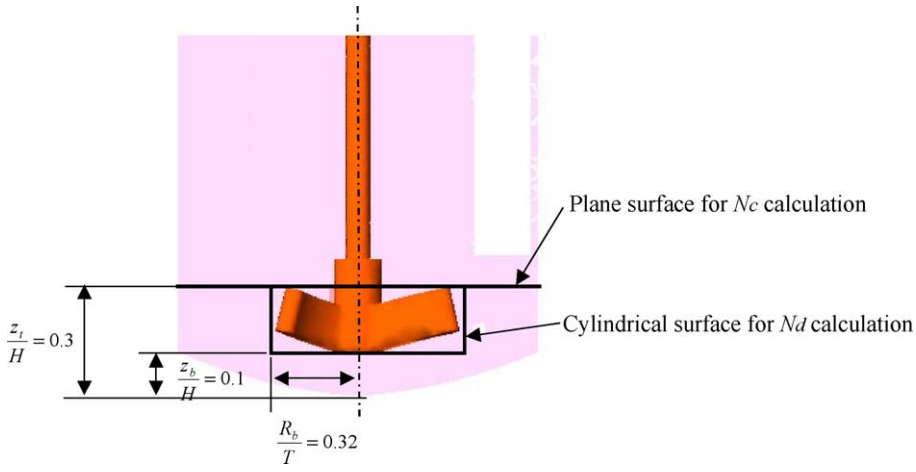

Fig. 10. Surface used to calculate impeller flow number and secondary circulation flow number.

3.3.4. Secondary circulation flow comparison

Secondary circulation flow is responsible for convective mixing within the tank. It is defined as the flux directed upward w_{up} defined in Eq. (1) across a reference section normal to the rotation axis. The surface of the normalised vertical distances $z/H = 0.3$ was selected, which is the same as the top surface of the cylinder used to calculate the pumping capacity shown in Fig. 10. The secondary circulation flow is used to scale the top–bottom turnover and mixing time. The secondary circulation flow is represented by the dimensionless secondary circulation flow number as

$$N_c = \frac{w_{up}}{\rho N D^3} \tag{8}$$

A comparison of secondary circulation flow number at different scales is also given in Table 3. The secondary circulation flow is almost independent of Reynolds number according to the simulations for different scale vessels: around 0.54 at the 0.5 l vessel, 0.57 at the 2 l vessel and 0.52 at the 20 l vessel. As the secondary circulation flow number is constant over a range of vessel scales, the mixing time only depends on the impeller speed and fluid volume in the vessel.

3.4. Flow field comparison

The flow number N_d and secondary circulation flow number N_c give an overall view of fluid dynamic behaviour of the vessel, which can be used to evaluate the efficiency of an impeller, and they are determined by the flow pattern in the vessel. From the above comparisons, it can be seen that for these three geometrically similar vessels the flow numbers and secondary circulation flow numbers are nearly the same, suggesting that the flow patterns should be similar in these three scale vessels, which have been examined by a comparison of the flow patterns at different scales. Fig. 11 shows the flow pattern comparison for different scale vessels at a Reynolds number of 5.0×10^4 on a plane across the impeller shaft and baffle. The vectors represent the resultant axial and radial velocities normalised by impeller blade tip speeds and averaged over one revolution of simulated rotation angle of the impeller. The comparison shows that the same fluid flow fields are created in each scale vessel. Features of the fluid flow field include: opposite the baffle, there is a big circulation from the vessel bottom to the middle of the vessel whose centre is about $0.3H$; on the right side of the impeller, there are two circulations, one is below the baffle and the other is immediately above the bottom.

Table 3
Parameter comparison

No.	*Re*	N_p			N_d			η			N_c		
		0.5 l	2 l	20 l	0.5 l	2 l	20 l	0.5 l	2 l	20 l	0.5 l	2 l	20 l
1	4.5×10^3	1.22	1.22	1.1	0.63	0.58	0.46	0.52	0.47	0.42	0.59	0.57	0.52
2	1.0×10^4	1.08	1.16	1.07	0.59	0.57	0.44	0.55	0.49	0.41	0.56	0.59	0.52
3	1.5×10^4	1.07	1.17	1.08	0.58	0.56	0.45	0.54	0.48	0.42	0.55	0.58	0.52
4	5.0×10^4	1.07	1.15	1.06	0.55	0.53	0.45	0.52	0.47	0.42	0.55	0.56	0.52
5	7.6×10^4	1.07	1.16	1.06	0.55	0.53	0.44	0.52	0.46	0.42	0.54	0.57	0.52
6	1.0×10^5	1.07	1.16	1.06	0.55	0.53	0.44	0.52	0.46	0.42	0.54	0.57	0.52
7	1.5×10^5	1.07	1.16	1.06	0.55	0.53	0.45	0.51	0.46	0.42	0.54	0.57	0.52
8	2.5×10^5	1.07	1.16	1.06	0.55	0.53	0.45	0.51	0.46	0.42	0.54	0.57	0.52

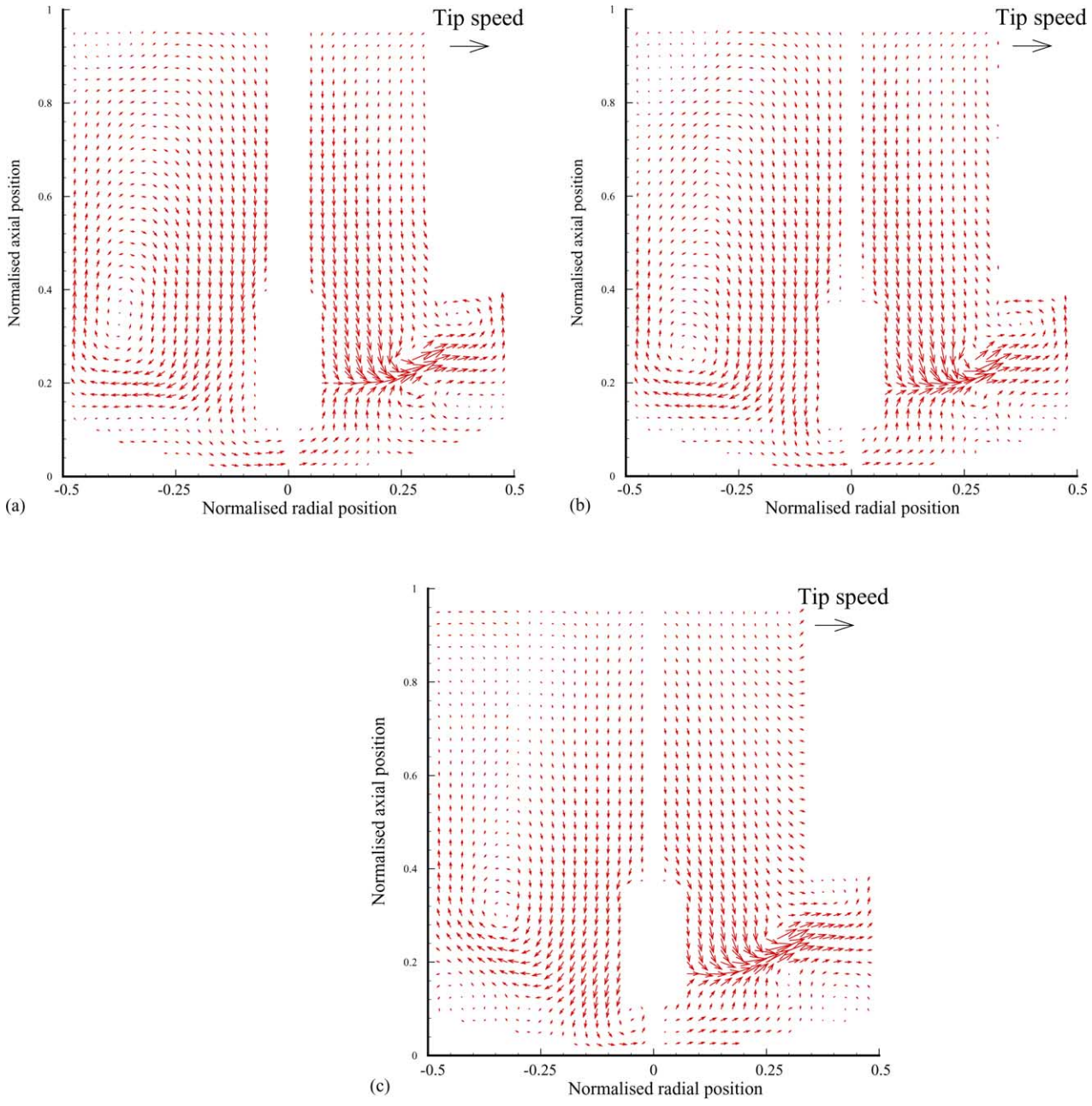

Fig. 11. Flow pattern comparison for different scale vessels: (a) 0.5 l vessel; (b) 2 l vessel; (c) 20 l vessel.

4. Discussion and conclusions

Scale up of mixing tanks from laboratory to industrial size is important and the selection of a laboratory scale vessel for experiments may directly affect the optimisation of an industrial scale reactor. The aim of this study was to compare the macro performance indicators, power number, discharge flow number, secondary circulation flow number and pumping efficiency for three different laboratory scale stirred vessels of 0.5, 2 and 20 l. The stirred vessel with a retreat curve impeller and single cylindrical baffle chosen in this study is especially used for crystallisation study in our laboratory. The scale up study is based on the three-dimensional, time-dependent CFD simulations.

The CFD results have been validated using LDA measurements and empirical power consumption prediction by Nagata, showing that CFD simulations are suitable for scale up study. The scale up study results show that for geometrically similar stirred reactors the discharge flow number, secondary circulation flow number and pumping efficiency slightly decrease with increasing vessel size, however, the power number is nearly constant for each scale vessel except that it increases slightly at low Reynolds number. The study results indicate that the selection of a laboratory scale ves-

sel has little effect on the macro mixing performance for the optimisation of the configurations and operating conditions of an industrial scale reactor, provided fully turbulent flow is achieved.

Apart from macro mixing performance, micro mixing performance indicators such as turbulent kinetic energy and local energy dissipation rate are also important in processes, especially for crystallisation. The scale up study for micro mixing performance is ongoing.

Acknowledgements

This work has been carried out as part of Chemicals Behaving Badly Phase 2, a collaborative project funded by EPSRC (Grant GR/R43877) together with support from an industrial consortium including ANSYS Europe Ltd., AstraZeneca, Bede Scientific Instruments Ltd., BNFL, Clairet Scientific Ltd., GlaxoSmithKline, HEL Ltd., Malvern Instruments, Pfizer and Syngenta. The academic partners are Leeds, Heriot Watt and Newcastle Universities. We gratefully acknowledge all these sponsors and all members of this academic/industrial team and the industrial coordinator L.J. Ford.

References

[1] J.Y. Oldshue, Geometric relationships for scale-up of diverse mixing processes, AIChE Symposium Series No. 293, vol. 89, 1993, pp. 159–163.
[2] V.V. Ranade, An efficient computational model for simulating flow in stirred vessels: a case of Rushton turbine, Chem. Eng. Sci. 52 (24) (1997) 4473–4484.
[3] V.V. Ranade, M. Perrard, N.L. Sauze, C. Xuereb, J. Bertrand, Trailing vortices of Rushton turbine: PIV measurements and CFD simulations with snapshot approach, Chem. Eng. Res. Des. 79 (2001) 3–12.
[4] Z. Jaworski, K.N. Dyster, A.W. Nienow, The effect of size, location and pumping direction of Piched blade turbine impellers on flow patterns: LDA measurements and CFD predictions, Chem. Eng. Res. Des. 79 (2001) 887–894.
[5] A.D. Harvey, S.E. Rogers, Steady and unsteady computation of impeller-stirred reactors, AIChE J. 42 (10) (1996) 2701–2712.
[6] W. Bujalski, Z. Jaworski, A.W. Nienow, CFD study of homogenization with dual Rushton turbines—comparison with experimental results, Part II: the multiple reference frame, Chem. Eng. Res. Des. 80 (2002) 97–104.
[7] G. Montante, K.C. Lee, A. Brucato, M. Yianneskis, Numerical simulations of the dependency of flow pattern on impeller clearance in stirred vessels, Chem. Eng. Sci. 56 (2001) 3751–3770.
[8] G. Montante, K.C. Lee, A. Brucato, M. Yianneskis, Experiments and predictions of the transition of the flow pattern with impeller clearance in stirred tanks, Comput. Chem. Eng. 25 (2001) 729–735.
[9] A. Serra, M. Campolo, A. Soldati, Time-dependent finite-volume simulation of the turbulent flow in a free-surface CSTR, Chem. Eng. Sci. 56 (2001) 2715–2720.
[10] A.D. Harvey, C.K. Lee, S.T. Rogers, Steady-state modelling and experimental measurement of a baffled impeller stirred tank, AIChE J. 41 (10) (1995) 2177–2186.
[11] A. Bakker, K.J. Myers, R.W. Ward, C.K. Lee, The laminar and turbulent flow pattern of a pitched blade turbine, Chem. Eng. Res. Des. 74 (1996) 485–491.
[12] M. Campolo, A. Paglianti, A. Soldati, Fluid dynamic efficiency and scale-up of a retreated blade impeller CSTR, Ind. Eng. Chem. Res. 41 (2002) 64–172.
[13] M. Campolo, A. Soldati, Appraisal of fluid dynamic efficiency of retreated-blade and turbofoil impellers in industrial-size CSTRs, Ind. Eng. Chem. Res. 41 (2002) 1370–1377.
[14] A. Brucato, M. Ciofalo, F. Grisafi, G. Micale, Numerical prediction of flow fields in baffled stirred vessels: a comparison of alternative modelling approached, Chem. Eng. Sci. 53 (21) (1998) 3653–3684.
[15] S. Nagata, Mixing: Principles and Application, Kodansha, Tokyo, Japan, 1975 (Chapter 1), pp. 31–59.
[16] F.R. Menter, Two-equation eddy-viscosity turbulence models for engineering applications, AIAA J. 32 (8) (1994) 269–289.
[17] M. Li, G. White, D. Wilkinson, K.J. Roberts, LDA measurements and CFD modelling of a stirred vessel with a retreat curve impeller, Ind. Eng. Chem. Res. 43 (2004) 6534–6547.
[18] W. Bujalski, A.W. Nenow, S. Chatwin, M. Cooke, The dependency on scale and material thickness of power number of different impeller types, in: Proceedings of the International Conference on Mechanical Agitation, vol. 1, ENS, Association of Chemical Engineers, Toulouse, France, 1986, p. 37.